

Revealing Floating-Point Accumulation Orders in Software/Hardware Implementations

Peichen Xie
Microsoft Research

Yanjie Gao
Microsoft Research

Yang Wang
Microsoft Research

Jilong Xue
Microsoft Research

Abstract

Accumulation-based operations, such as summation and matrix multiplication, are fundamental to numerous computational domains. However, their accumulation orders are often undocumented in existing software and hardware implementations, making it difficult for developers to ensure consistent results across systems. To address this issue, we introduce FPRev, a diagnostic tool designed to reveal the accumulation order in the software and hardware implementations through numerical testing. With FPRev, developers can identify and compare accumulation orders, enabling developers to create reproducible software and verify implementation equivalence.

FPRev is a testing-based tool that non-intrusively reveals the accumulation order by analyzing the outputs of the tested implementation for distinct specially designed inputs. Employing FPRev, we showcase the accumulation orders of popular libraries (such as NumPy and PyTorch) on CPUs and GPUs (including GPUs with specialized matrix accelerators such as Tensor Cores). We also validate the efficiency of FPRev through extensive experiments. FPRev exhibits a lower time complexity compared to the basic solution. FPRev will be open-sourced on GitHub.

1 Introduction

Today, floating-point computations are ubiquitous, with accumulation-based operations (AccumOps) such as summation, dot products, matrix-vector multiplications, and matrix multiplications playing fundamental roles in various domains. However, no general specification dictates the accumulation orders of AccumOps. Without well-defined requirements, AccumOps are implemented differently across software and hardware, leading to inconsistencies due to the non-associativity of floating-point addition [29]. For example, the half-precision (float16) sum of 0.5, 512, and 512.5 depends on the accumulation order: $(0.5 + 512) + 512.5 = 1025$, while $0.5 + (512 + 512.5) = 1024$. Consequently, varying AccumOp implementations yield different results, complicating reproducibility in software development.

Numerical reproducibility is critical in rigorous scenarios like finance [23, 24], where even minor inconsistencies in financial data are unacceptable. Software without verified numerical reproducibility is deemed risky or disqualified when applied to the rigorous scenarios. Unfortunately, with the rapid evolution of heterogeneous hardware and the fast iteration of diverse software stacks, reproducibility of AccumOps has become increasingly challenging. Existing implementations rarely disclose their accumulation orders, hindering reproducible AccumOp development.

We propose FPRev, a diagnostic tool to help developers identify how AccumOps are implemented in software and hardware. FPRev reveals the accumulation order of an AccumOp implementation (AccumImpl) through numerical testing. This enables developers to reproduce an AccumImpl on a new system by using the revealed accumulation order as a specification and verify equivalence between two implementations by comparing their accumulation orders.

As a case study, we use FPRev to analyze popular numerical libraries on diverse hardware, uncovering their undocumented and undisclosed accumulation orders. On different CPUs, we apply FPRev to the NumPy library [9]. On different GPUs, we apply FPRev to the PyTorch library [22]. The results indicate that NumPy’s summation functions are implemented equivalently across CPUs, and the same holds for PyTorch’s summation functions across GPUs. However, other AccumOps relying on BLAS (Basic Linear Algebra Subprograms) backends like Intel MKL [13], OpenBLAS [21], and NVIDIA cuBLAS [20] exhibit non-reproducible behavior.

FPRev also visualizes the order with the summation tree, i.e., a full binary tree representing how an AccumImpl performs summation, to guide development. For example, Figure 1 illustrates NumPy’s summation of 32 single-precision (float32) numbers. It divides the 32 numbers into 8 ways, accumulates the summands with a stride of 8 on each way, and sums up the 8 ways together using pairwise summation. This 8-way accumulation order is friendly to CPU’s SIMD instructions. With this information, it is easy to replicate NumPy’s numerical behavior in a new implementation.

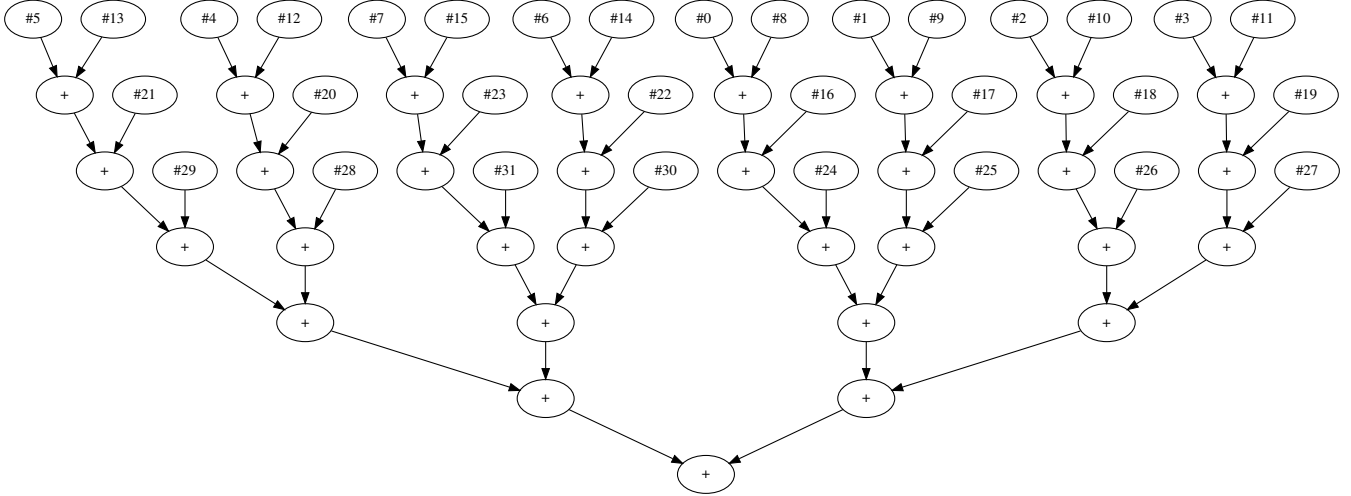


Figure 1: Visualizing the accumulation order of Numpy’s summation function for $n = 32$ single-precision numbers with a summation tree. The numbers on the leaf nodes denote the indexes in the input.

Design overview. Determining the accumulation order of an AccumImpl is a challenging task. Static methods, such as analyzing the source code, are cumbersome and inapplicable to black-box implementations and compiler optimization. Dynamic methods, like scrutinizing the runtime traces, lack an automatic tool to analyze the traces. In addition, many software or hardware implementations are parallel, making the analysis more challenging.

We address these challenges through non-intrusive testing. Recall the example where $(0.5 + 512) + 512.5 = 1025$ and $0.5 + (512 + 512.5) = 1024$ in half precision. Different accumulation orders yield distinct results, making it possible to deduce the order from numerical outputs. However, the number of all possible accumulation orders is exponential, making the time complexity of the naive brute-force solution (NaiveSol) impractical.

To achieve practical time complexity, we propose a basic solution called BasicFPRev that uses specially designed inputs to facilitate the distinguishing process. We take the summation function for example. First, BasicFPRev set all n summands to 1.0. Then, two of the summands are replaced by a very large number (denoted by M) and its negative ($-M$), where M satisfies $(n - 2) + M = M$. The summation output corresponds to an integer between 0 and $n - 2$, depending on when M or $-M$ cancel each other during the accumulation. Specifically, when $\pm M$ is added to other numbers, it remains $\pm M$; when M is added to $-M$, it results in 0; after that, the remaining summands are accumulated without rounding errors because they are all 1.0. Therefore, the output equals the number of summands accumulated after $M + (-M)$.

BasicFPRev leverages this information to construct the summation tree. Using i and j to denote the indexes of M or $-M$ in the input, we note that the operation $M + (-M)$ corresponds to the lowest common ancestor (LCA) of node

$\#i$ and $\#j$ in the summation tree, and the number of leaf nodes under the LCA equals n minus the summation output. Based on this finding, BasicFPRev enumerates i and j , collects the output for the corresponding input, and infers the size of subtree rooted at the LCA of node $\#i$ and $\#j$. BasicFPRev then constructs the summation tree bottom-up, starting with subtrees of two leaf nodes and progressively building larger subtrees until the entire tree is generated.

Based on BasicFPRev, FPRev further reduces time complexity by eliminating redundancy, and adds support for matrix accelerators such as Tensor Cores on recent NVIDIA GPUs [17]. Matrix accelerators are specialized hardware units on GPUs for high-performance matrix multiplication, but they perform non-standard multi-term fused summations [7]. FPRev models their accumulation orders using a multiway tree, where a node with multiple children represents a multi-term fused summation for a group of summands. The summands are aligned and truncated before they are accumulated, as if they are added in finite-precision fixed-point arithmetic.

FPRev has a time complexity of $\Omega(nt(n))$ and $O(n^2t(n))$, where $t(n)$ is the time complexity of the tested AccumImpl. This shows a significant improvement over the $O(4^n/n^{3/2} \cdot t(n))$ complexity of NaiveSol and the $\Theta(n^2t(n))$ complexity of BasicFPRev. Experimental results confirm FPRev’s efficiency and scalability across diverse AccumOp implementations on three CPUs and three GPUs with distinct architectures.

In summary, the contributions of this paper include:

1. Design and development of FPRev: we introduce FPRev, a diagnostic tool that non-intrusively reveals the accumulation order of accumulation-based operations implemented in different software and hardware, enabling developers to verify equivalence and maintain numerical reproducibility between implementations.

2. Empirical analysis of popular implementations: We demonstrate FPREv’s capabilities by analyzing accumulation orders in popular libraries (e.g., NumPy and PyTorch) across CPUs and GPUs, providing reproducibility insights in backend implementations.
3. Algorithmic innovation: we describe the algorithm of FPREv for revealing accumulation orders and constructing summation trees, refine the algorithm to reduce time complexity, and extend it to handle modern GPU matrix accelerators (e.g., NVIDIA Tensor Cores), modeling their multi-term fused summation using multiway trees.
4. Performance evaluation: we evaluate FPREv’s efficiency through comprehensive experiments, test diverse AccumOps implementations on various CPUs and GPUs, and demonstrate significant performance improvements over naive and basic solutions.

2 Related work

2.1 AccumOp implementations

2.1.1 On canonical CPUs and GPUs

Accumulation-based operations (AccumOps) are implemented diversely on modern systems. On most CPUs and GPUs, implementations use standard IEEE-754 addition or fused multiply-add (FMA) arithmetic [12] to accumulate floating-point numbers. However, they may perform accumulations in different orders without explicitly disclosing those orders.

First, there is diverse numerical software, including BLAS libraries such as Intel MKL [13] and NVIDIA cuBLAS [20], Python libraries such as NumPy [9] and PyTorch [22], and domain-specific compilers such as Numba [15] and Triton [28]. These libraries are developed without a unified specification, making it difficult to guarantee consistent accumulation orders.

Second, the same software may behave differently across different hardware. Different CPUs and GPUs vary in architecture, number of cores, SIMD width, cache size, etc. Consequently, for performance optimization, software may adjust the accumulation order based on the specific hardware characteristic. Although order-independent algorithms have been proposed [4–6], which ensure consistent results regardless of the accumulation order, they are highly inefficient and thus rarely used in industry.

Our tool FPREv supports the AccumOp implementations on canonical CPUs and GPUs and can reveal their undisclosed accumulation orders.

2.1.2 On matrix accelerators

Matrix accelerators [17, 25] are specialized hardware components in modern GPUs designed for high-performance matrix

multiplication. Developers can implement matrix multiplications using the APIs of matrix accelerators [19]. However, the numerical behavior and accumulation order of the APIs are undocumented and inconsistent across different GPUs.

FPREV supports the AccumOp implementations based on matrix accelerators and can reveal their undisclosed accumulation orders.

2.2 Revelation of numerical behaviors

FPREV achieves non-intrusive revelation of accumulation orders through numerical testing. Prior works [7, 16] have also employed numerical testing to study the numerical behavior of matrix accelerators. They design “corner cases” as test inputs and analyze the numerical behavior based on the outputs. They find that for float64 on NVIDIA Tensor Cores and AMD Matrix Cores, the matrix multiplication instruction is based on a chain of standard FMA arithmetic. In contrast, other instructions use a non-standard arithmetic where multiple terms (the exact number depends on the hardware) are accumulated after alignment and truncation.

FPREV is a general tool that applies to AccumOp implementations, including those based on matrix accelerators, while prior works focus exclusively on specific hardware.

2.3 Numerical reproducibility engineering

The inconsistent AccumOp implementations pose significant issues in numerical reproducibility [2, 29]. To help developers debug the issues, several testing-based tools have been proposed. For example, Varsity [14] uses randomized testing to verify equivalence between implementations. Tools like pLiner [8] and its follow-up [18] employ differential testing to pinpoint non-reproducible parts of a program. In contrast, FPREv uses a deterministic testing method to identify the accumulation order of AccumOps.

Early works [10, 27] have emphasized the importance of reproducible AccumOps for ensuring numerical stability but lack practical solutions. A preliminary approach [1] adopts the aforementioned order-independent algorithm [5] to ensure reproducibility, but suffers from its inefficiency. In contrast, FPREv offers a more practical solution: replicating the accumulation order of existing efficient implementations.

3 Problem statement

3.1 Motivation

Accumulation-based operations (AccumOps) are fundamental in floating-point computing, but most implementations do not specify their accumulation orders. This lack of transparency motivates us to design a tool for revealing the accumulation order.

An example application of the tool is in developing reproducible AccumOps, which are key to software reproducibility and stability [10, 27]. Developers must ensure that the accumulation order remains consistent across systems to maintain the reproducibility of AccumOps. If developers can determine the accumulation order, they can use it as a specification to guide their development process. In addition, when porting software to a new system, developers need a rigorous way to verify the equivalence of AccumOps between two systems. This can be achieved by comparing the accumulation orders of the AccumOps implemented on two systems.

3.2 Problem definition

For an AccumOp implementation (AccumImpl), we aim to design a diagnostic tool to reveal its accumulation order. For brevity, we focus on the summation function in the following discussion, since other AccumOps can be abstracted as calls to the summation function with the intermediate results as inputs. For example, dot product $\mathbf{x} \cdot \mathbf{y}$ can be treated as $\sum_{i=0}^{n-1} x_i y_i$. Thus, solutions for the summation function can be naturally applied to other AccumOps.

We formulate the summation operation as follows. The floating-point addition is performed $n - 1$ times in a predetermined order to calculate the sum of n floating-point numbers. We assume that the accumulation order is unknown but is uniquely determined by the given implementation on specific hardware. Therefore, randomized implementations and those where the order depends on the values of the summands are out of scope.

The problem is how to reveal the accumulation order in a summation implementation, denoted by SUMIMPL. Specifically, the input of our revelation algorithm is SUMIMPL and the number of summands n . The output of the algorithm is the accumulation order of SUMIMPL.

Strictly speaking, the accumulation order is represented by a computational graph called the summation tree, which is a rooted full binary tree with n leaf nodes and $n - 1$ inner nodes. Each addition operation corresponds to an inner node, which represents the sum of this operation. The two children of the node represent the two summands of this operation. For example, Figure 1 depicts the accumulation order of Numpy’s summation function for $n = 32$ single-precision numbers.

3.3 Inefficiency of the naive solution

We now introduce a naive solution (NaiveSol) to the problem, which is based on brute-force search. We design a recursive algorithm to enumerate every possible accumulation orders. For each order, we verify its correctness through randomized testing. Specifically, we generate multiple random inputs, compute the sums in the current order, and compare the results with those from SUMIMPL. If the results match, we accept the order.

The time complexity of NaiveSol is $O(4^n/n^{3/2} \cdot t(n))$, as the number of all possible orders is the $(n - 1)$ -th Catalan number $C_{n-1} = \frac{(2n-2)!}{n!(n-1)!} = O(4^n/n^{3/2})$. Here, $t(n)$ represents the time complexity of SUMIMPL. In addition to being inefficient, NaiveSol is not fully reliable because different orders can produce the same output for certain inputs. Although the probability is low and reliability can be improved by increasing the number of test inputs, a deterministic solution with full reliability is preferable, as we will achieve next.

4 Basic polynomial-time solution

The exponential complexity of the naive solution is highly impractical. To address the issue, we present our basic solution called BasicFPRev for revealing the accumulation order, which reduces the time complexity to polynomial. We design an algorithm to determine the accumulation order from the numerical results of the tested summation implementation (SUMIMPL) for specially designed testing inputs. The following parts detail the three steps of the algorithm.

4.1 Step 1: designing testing inputs

To facilitate distinguishing the accumulation order, we leverage the swamping phenomenon of floating-point addition [11]. When two floating-point numbers differing by many orders of magnitude are added, the smaller number is swamped and makes no contribution to the sum. For example, $2^{24} + 1$ equals 2^{24} in single-precision (float32) arithmetic.

To induce and utilize this phenomenon, we construct various “masked all-one arrays” as testing inputs. Specifically, let n denote the number of summands, and let SUMIMPL represent an summation implementation with a predetermined but unknown accumulation order. Let M be a very large floating-point number that readily induces the swamping phenomenon. For example, we set $M = 2^{127}$ for float32 or $M = 2^{1023}$ for float64. Then, we define a masked all-one array $A^{i,j}$ as $A^{i,j} = (A_0^{i,j}, A_1^{i,j}, \dots, A_{n-1}^{i,j})$ such that

$$A_k^{i,j} = \begin{cases} M & \text{if } k = i \\ -M & \text{if } k = j \\ 1.0 & \text{otherwise} \end{cases}$$

where i and j denote the indexes of M and $-M$ in the array. In $A^{i,j}$, there exist exactly one M and one $-M$, with all other elements being 1.0.

We use $\pm M$ as masks. Specifically, $M + \sigma = M$ and $-M + \sigma = -M$ hold for $0 \leq \sigma \leq n - 2$ in floating-point arithmetic, if $n \ll M$. Therefore, in SUMIMPL($A^{i,j}$), adding any summand or intermediate sum (except M and $-M$ themselves) to $\pm M$ yields $\pm M$. In other words, M and $-M$ can mask the summands or intermediate sums added to them.

As a result, the output of $\text{SUMIMPL}(A^{i,j})$ depends on the accumulation order and we can distinguish the accumulation order from the output. For example, given $n = 3$ and $A^{0,1} = (M, -M, 1)$, sequential summation $M + (-M) + 1$ corresponds to 1, stride summation $M + 1 + (-M)$ corresponds to 0, and reverse summation $1 + (-M) + M$ corresponds to 0. If the output equals 1, then we can infer the accumulation order is sequential summation. If the output equals 0, we can determine the exact accumulation order by further testing with $A^{0,2}$ as the input.

4.2 Step 2: analyzing the accumulation order from the outputs

To analyze the accumulation order, we call SUMIMPL with $n(n-1)/2$ inputs, i.e., $A^{i,j}$ for $0 \leq i < j < n$. Each output reveals information about the accumulation order. Specifically, since $\pm M$ mask the summands or intermediate sums added to them, these numbers make no contribution to the sum. In contrast, only those summands not masked by $\pm M$ contribute to the sum. Therefore, the output equals the sum of these summands. Since each of the summands equals 1.0, the output equals the number of the summands not masked by $\pm M$:

$$n_{\text{not masked}}^{i,j} = \text{SUMIMPL}(A^{i,j}).$$

Then, we can also obtain the number of the summands masked by $\pm M$ by calculating $n_{\text{masked}}^{i,j} = n - 2 - n_{\text{not masked}}^{i,j}$.

How does this information relate to the order, or specifically, the summation tree? Recall that i and j denote the positions of the masks, represented by node $\#i$ and $\#j$ in the summation tree. **We note that the neutralization of the two masks (i.e., the addition operation $M + (-M) = 0$) corresponds to the lowest common ancestor (LCA) of node $\#i$ and $\#j$.** Then, observing the subtree rooted at the LCA, we find that all the summands masked by $\pm M$ are in the subtree, and all the summands not masked by $\pm M$ are out of the subtree. Therefore, the number of leaf nodes in the subtree (representing the size of the subtree) equals $n - n_{\text{not masked}}^{i,j}$, denoted by

$$l^{i,j} = n - n_{\text{not masked}}^{i,j} = n - \text{SUMIMPL}(A^{i,j}).$$

For brevity, we use $l^{i,j}$ to denote “the number of leaf nodes in the subtree rooted at the LCA of node $\#i$ and $\#j$ ” in the rest of the paper.

Take Algorithm 1 as an example SUMIMPL , whose accumulation order is depicted in Figure 2. If $i = 2$ and $j = 4$, then the array $A^{2,4}$ is $(1, 1, M, 1, -M, 1, 1, 1)$. Computing the sum of $A^{2,4}$ with the example SUMIMPL , the 3rd summand and the intermediate sum of the 0th and 1st summands are masked by M (the 2nd summand); the 5th summand is masked by $-M$ (the 4th summand). Therefore, in total, $n_{\text{masked}}^{2,4} = 4$. In contrast, the 6th and 7th summands and their intermediate sum are not added to M or $-M$, so $n_{\text{not masked}}^{2,4} = \text{SUMIMPL}(A^{2,4}) = 2$.

Algorithm 1 An example summation implementation.

```
float sum = 0;
for (int i=0; i<8; i+=2)
    sum += a[i] + a[i+1];
```

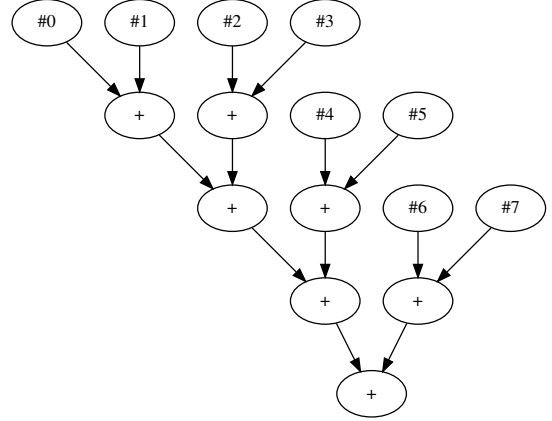


Figure 2: The summation tree of Algorithm 1. The numbers on the leaf nodes denote the indexes in the input.

The LCA of node $\#2$ and $\#4$ is the grandparent node of node $\#4$, as shown in 2. It corresponds to the neutralization of the 2nd summand M and the 4th summand $-M$, i.e., $M + (-M) = 0$. Within the subtree rooted there, there are node $\#0$, $\#1$, $\#2$, $\#3$, $\#4$, and $\#5$ (6 leaf nodes in total), corresponding to the two masks and the summands masked by them. In contrast, node $\#6$ and $\#7$ (2 leaf nodes in total), which correspond to the summands not masked, are out of the subtree. Therefore, $l^{2,4} = 8 - 2 = 6$. Table 1 shows more examples of the output of $\text{SUMIMPL}(A^{i,j})$ and $l^{i,j}$ for Algorithm 1.

Table 1: The order-related information $l^{i,j}$ inferred from the outputs of Algorithm 1 with different masked all-one arrays $A^{i,j}$ as inputs.

i	j	Input: $A^{i,j}$	Output	$l^{i,j}$
0	1	$(M, -M, 1, 1, 1, 1, 1, 1)$	6	2
0	2	$(M, 1, -M, 1, 1, 1, 1, 1)$	4	4
0	3	$(M, 1, 1, -M, 1, 1, 1, 1)$	4	4
0	4	$(M, 1, 1, 1, -M, 1, 1, 1)$	2	6
0	5	$(M, 1, 1, 1, 1, -M, 1, 1)$	2	6
0	6	$(M, 1, 1, 1, 1, 1, -M, 1)$	0	8
0	7	$(M, 1, 1, 1, 1, 1, 1, -M)$	0	8
		...		
2	3	$(1, 1, M, -M, 1, 1, 1, 1)$	6	2
2	4	$(1, 1, M, 1, -M, 1, 1, 1)$	2	6
		...		

4.3 Step 3: generating the summation tree

With the information $L = \{(l^{i,j}, i, j)\}$ derived from the outputs, where $l^{i,j}$ represents the size of the subtree rooted at the LCA of node $\#i$ and $\#j$, generating the summation tree from L is a tree algorithm problem.

Our solution employs a bottom-up approach to construct the tree. First, we sort L in ascending order. For each $l^{i,j}$, we locate the root of the existing subtree containing node $\#i$ and the root of the existing subtree containing node $\#j$, and merge them by creating a new parent node for them. By repeating this process, we construct the entire summation tree, progressing from small subtrees to larger ones.

For example, consider the order-related information $L = \{(l^{i,j}, i, j)\}$ shown in Table 1. To generate the summation tree, we start by initializing the tree with eight disjoint nodes labeled 0 to 7. Then, examining the smallest value in L , we have $l^{0,1} = 2$. This implies that the subtree rooted at the LCA of node $\#0$ and $\#1$ should have 2 leaf nodes. Since the summation tree is a full binary tree, node $\#0$ and $\#1$ are exactly the two children of the root of this subtree. Therefore, we add a new node to the tree, label it with n plus the label of its left child (i.e., $n+0$ in this example), and add two edges from the two leaf nodes to the new node.

For $l^{2,3} = l^{4,5} = l^{6,7} = 2$, similarly, we can construct the subtree containing node $\#2$ and $\#3$, the subtree containing node $\#4$ and $\#5$, and the subtree containing node $\#6$ and $\#7$. Now, we have four subtrees of size 2, where the size of a subtree is represented by the number of leaf nodes in it.

Next, the smallest unexamined value in L is $l^{0,2} = 4$. This implies that the subtree rooted at the LCA of node $\#0$ and $\#2$ should have 4 leaf nodes. We note that node $\#0$ and $\#2$ are currently in two different subtrees (each has 2 leaf nodes), so we should merge the two subtrees. Therefore, we find the current roots of the subtrees containing node $\#0$ and $\#2$ respectively, i.e., node $\#i'$ and $\#j'$ where $i' = n+0$ and $j' = n+2$. Subsequently, we add a new node as the parent of node $\#i'$ and $\#j'$, label it with n plus the label of its left child, i.e., $n+i' = 2n+0$, and add two edges from node $\#i'$ and $\#j'$ to the new node.

For $l^{0,3} = 4$, we find that node $\#0$ and $\#3$ are already in the same subtree with 4 leaf nodes, so we just skip it. The same process is applied to $l^{1,2} = l^{1,3} = 4$. Now, we have a subtree with 4 leaf nodes and two subtrees with 2.

The next smallest unexamined value in L is $l^{0,4} = 6$, which implies that the subtree rooted at the LCA of node $\#0$ and $\#4$ should have 6 leaf nodes. Similarly, node $\#0$ and $\#4$ are currently in two different subtrees (one has 4 leaf nodes and the other has 2), so we should merge the two subtrees. Therefore, following the similar process, we find the current roots of the trees containing node $\#0$ and $\#4$ respectively, i.e., node $\#i'$ and $\#j'$ where $i' = 2n+0$ and $j' = n+4$. Subsequently, we create a new node as their parent (labelled as $n+i' = 3n+0$), and add two edges from node $\#i'$ and $\#j'$ to it.

For $l^{0,5} = 6$, we find that node $\#0$ and $\#5$ are already in the same subtree with 6 leaf nodes, so we skip it. The same process is applied to $i \in \{1, 2, 3\}$ and $j \in \{4, 5\}$. Now, we have a subtree of with 6 leaf nodes and a subtree of with 2.

Finally, in the similar way, the next smallest unexamined value in L is $l^{0,6} = 8$, which implies that the subtree rooted at the LCA of node $\#0$ and $\#6$ should have 8 leaf nodes. Since node $\#0$ and $\#6$ are currently in two different subtrees (one has 6 leaf nodes and the other has 2), we should merge the two subtrees. After we add the parent node of the current roots of the two subtrees and add the corresponding edges, the entire summation tree is generated.

To generalize and formulate the algorithm, we present BasicFPRev in Algorithm 2, where the GENERATETREE function encapsulates Step 3. It first initializes T with n disjoint nodes and no edges. Then, for each $l^{i,j}$, it finds the roots of the existing subtrees containing node $\#i$ and $\#j$. If they are identical, then the i -node $\#i$ and $\#j$ are already in the same subtree. Otherwise, it combines them. The FindRoot function can be implemented by the disjoint-set data structure, resulting in an amortized time complexity of $O(\alpha(n))$ [26], where $\alpha(n)$ is the inverse Ackermann function.

Algorithm 2 BasicFPRev: our basic solution for revealing the accumulation order.

Require: Implementation SUMIMPL and the number of summands n

Ensure: Summation tree of SUMIMPL

function BASICFPREV(SUMIMPL, n)

$L \leftarrow \emptyset$

for $i \leftarrow 0$ to $n-1$ **do**

for $j \leftarrow i+1$ to $n-1$ **do**

$A^{i,j} \leftarrow (1, 1, \dots, 1)$; $A_i^{i,j} \leftarrow M$; $A_j^{i,j} \leftarrow -M$

$l^{i,j} \leftarrow n - \text{SUMIMPL}(A^{i,j})$

$L \leftarrow L \cup \{(l^{i,j}, i, j)\}$

function GENERATETREE(L)

$T \leftarrow \emptyset$

for $(l^{i,j}, i, j) \in L$ in ascending order **do**

$i' \leftarrow T.\text{FindRoot}(i)$

$j' \leftarrow T.\text{FindRoot}(j)$

if $i' \neq j'$ **then**

$k \leftarrow i' + n$

 ▷ assign a new label

$T \leftarrow T \cup \{(i', k), (j', k)\}$

return T

return GENERATETREE(L)

4.4 Time complexity and correctness analysis

Let $t(n)$ denote the time complexity of SUMIMPL. The computation of L has a time complexity of $\Theta(n^2 t(n))$. In GENERATETREE, the time complexity of sorting $n(n-1)/2$ elements is $\Theta(n^2 \log n^2) = \Theta(n^2 \log n)$. Therefore, the time

complexity of GENERATETREE is $\Theta(n^2 \log n + n^2 \alpha(n)) = \Theta(n^2 \log n)$. Thus, the overall time complexity of BasicFPRev is $\Theta(n^2 t(n)) + \Theta(n^2 \log n) = \Theta(n^2 t(n))$.

The correctness of BasicFPRev is inherent in its design and can be proven as follows. For a given implementation SUMIMPL and n , we use T to denote the real summation tree and define $T' = \text{BASICFPREV}(\text{SUMIMPL}, n)$. Assuming $T \neq T'$, there must exist i and j such that $l_T^{i,j} \neq l_{T'}^{i,j}$. Now we construct $A^{i,j}$ and compute its sum in the order T and T' respectively, resulting in s and s' . Then, $s = n - l_T^{i,j} \neq s' = n - l_{T'}^{i,j}$. However, since $s = \text{SUMIMPL}(A^{i,j})$, then $l_{T'}^{i,j} = n - s' \neq n - s = n - \text{SUMIMPL}(A^{i,j})$. This contradicts the statement $l^{i,j} \leftarrow n - \text{SUMIMPL}(A^{i,j})$ in Algorithm 2. Therefore, the assumption $T \neq T'$ is false, so $T = T'$.

5 Algorithm improvement in FPRev

This section introduces the full version of our tool FPRev, which is evolved from our basic solution BasicFPRev detailed in Section 4. First, we refine the algorithm to reduce its time complexity. Second, based on the refined algorithm, we add support for multi-term fused summation, which is used by matrix accelerators, and finalize FPRev.

5.1 Reducing time complexity

5.1.1 Removing redundancy

By analyzing BasicFPRev, we observe that Algorithm 2 requires $n(n-1)/2$ different $(l^{i,j}, i, j)$ tuples, even though many values of $l^{i,j}$ are identical. However, only $n-1$ new nodes and $2(n-1)$ new edges are constructed. Since computing multiple $l^{i,j}$ by calling SUMIMPL is the primary source of the method's time complexity, reducing redundancy in $l^{i,j}$ (i.e., the cases corresponding to $i' = j'$ in Algorithm 2) can significantly improve efficiency.

To achieve this, we calculate $l^{i,j}$ on demand. Specifically, we do not calculate all $l^{i,j}$ ahead of the tree generation. Instead, we directly start to generate the summation tree, and calculate $l^{i,j}$ when needed. Following the bottom-up idea, we still construct subtrees from leaf to root.

Step 1. We use the set $I = \{0, 1, \dots, n-1\}$ to denote the labels of the leaf nodes for which we are going to construct a summation tree. Let i represent the leaf node with the smallest label in I . The sibling node of node $\#i$ is either a leaf node or an inner node. If it is a leaf node, there exists a unique j such that $l^{i,j} = 2$. Otherwise, if it is an inner node, then $l^{i,j} > 2$ for all j such that $j \neq i$. Therefore, to distinguish the two cases, we need to calculate $l^{i,j}$ for all other js , denoted by the set $L_i = \{l^{i,j} : j \in I - \{i\}\}$. We examine the minimum value in L_i , which is denoted by $l = \min(L_i)$.

If l equals 2, let j be the one that satisfies $l^{i,j} = 2$. Then, node $\#j$ is the sibling node of node $\#i$, so we add a new node

to the tree, and add two edges from node $\#i$ and $\#j$ to the new node. Now, the currently constructed subtree has 2 leaf nodes.

Otherwise, if l is larger than 2, the sibling node of node $\#i$ must be an inner node. The subtree rooted at this inner node must have $l-1$ leaf nodes. Let $J_l = \{j : j \in I - \{i\} \wedge l^{i,j} = l\}$. Then, the number of members of J_l must be $l-1$, and the members of J_l are exactly the leaf nodes of this subtree. This can be proven by contradiction. Now, constructing this subtree is a subproblem for the set J_l . Suppose that we have constructed this subtree by a recursive algorithm. We shall add a new node to the tree, and add edges from node $\#i$ and the root node of this subtree to the new node. Now, the currently constructed subtree has l leaf nodes.

Summarizing the two cases, we can treat both cases as the same pattern: finding $J_l = \{j : j \in I - \{i\} \wedge l^{i,j} = l\}$ and solving the subproblem for J_l . The first case ($|J_l| = 1$) just leads to the stop condition of the recursion ($|I| = 1$).

Step 2. Now we have constructed a subtree with l leaf nodes. Let r be the root of this subtree. Similarly, to find the sibling node of r , we examine the minimum value in the rest of L_i , which is denoted by l' here. Then, we solve the subproblem for $J_{l'} = \{j : j \in I - \{i\} \wedge l^{i,j} = l'\}$, and get a subtree whose leaf nodes are $J_{l'}$. The root of the subtree, whether a leaf node or an inner node, is the sibling node of r . Therefore, we shall add a new node to the tree, and add edges from r and the root node of the subtree to the new node. Now, the currently constructed subtree has l' leaf nodes.

Remaining steps. We repeat the above step until all values in L_i are examined and the entire tree is constructed. We implement this method with a recursive algorithm, as shown in Algorithm 3.

5.1.2 Demonstration with example

Consider the example SUMIMPL in Algorithm 1, whose summation tree is illustrated in Figure 2. We call Algorithm 3 with this SUMIMPL and $n = 8$. First, the set of leaf nodes is $I = \{0, 1, \dots, 7\}$, where the smallest label is $i = 0$. Next, the set $L_i = \{l^{i,j} : j \in I - \{i\}\} = \{2, 4, 4, 6, 6, 8, 8\} = \{2, 4, 6, 8\}$ is computed. Examining the smallest value in L_i , we have $l = 2$ and $J_l = \{j : j \in I - \{i\} \wedge l^{i,j} = l\} = \{1\}$. Therefore, BUILDSTREE($\{1\}$) is called, reaching the stop condition. Then, the subtree with node $\#0$ and $\#1$ as its leaf nodes is constructed. The root of this subtree is denoted by r .

Next, examining the smallest value in the rest of L_i , we have $l = 4$ and $J_l = \{j : j \in I - \{i\} \wedge l^{i,j} = l\} = \{2, 3\}$. Therefore, BUILDSTREE($\{2, 3\}$) is called, where we have $I = \{2, 3\}$, $i = 2$, and $L_i = \{2\}$, and BUILDSTREE($\{3\}$) is called there. BUILDSTREE($\{2, 3\}$) returns the subtree with node $\#2$ and $\#3$ as its leaf nodes. We then designate its root as the sibling node of r , and construct the parent node of this root and r . Then, the subtree with node $\#0, \#1, \#2,$ and $\#3$ as its leaf nodes is constructed. r is updated by the root of this subtree.

The next smallest value is $l = 6$. We have $J_l = \{4, 5\}$. Sim-

Algorithm 3 Refinement of BasicFPRev (Algorithm 2).

Require: Implementation SUMIMPL and the number of summands n

Ensure: Summation tree of SUMIMPL

```
function BASICFPREVREFINED(SUMIMPL,  $n$ )
  function BUILDSUBTREE( $I$ )
     $T \leftarrow \emptyset$ 
    if  $|I| = 1$  then                                ▷ stop condition
      return  $T$ 
     $i \leftarrow \min(I)$ ;  $L_i \leftarrow \emptyset$ 
    for  $j \in I - \{i\}$  do                               ▷ calculate  $l^{i,j}$  on demand
       $A^{i,j} \leftarrow (1, 1, \dots, 1)$ ;  $A_i^{i,j} \leftarrow M$ ;  $A_j^{i,j} \leftarrow -M$ 
       $l^{i,j} \leftarrow n - \text{SUMIMPL}(A^{i,j})$ 
       $L_i \leftarrow L_i \cup \{l^{i,j}\}$ 
     $r \leftarrow i$                                        ▷ current root of the subtree
    for  $l \in L_i$  in ascending order do
       $J_l \leftarrow \{j : j \in I - \{i\} \wedge l^{i,j} = l\}$ 
       $T' \leftarrow \text{BUILDSUBTREE}(J_l)$ 
       $T \leftarrow T \cup T'$ 
       $T \leftarrow T \cup \{(r, r+n), (\text{GetRoot}(T'), r+n)\}$ 
       $r \leftarrow r+n$ 
    return  $T$ 
  return BUILDSUBTREE( $\{0, 1, \dots, n-1\}$ )
```

ilarly, BUILDSUBTREE($\{4, 5\}$) is called, and it returns the subtree with node #4 and #5 as its leaf nodes. We merge its root with r , and construct the subtree with node #0, #1, #2, #3, #4, and #5 as its leaf nodes. r is updated by the root of this subtree.

Finally, $l = 8$ and $J_l = \{6, 7\}$. BUILDSUBTREE($\{6, 7\}$) is called, and it returns the subtree with node #6 and #7 as its leaf nodes. We merge its root with r . Then the entire tree is constructed.

5.1.3 Time complexity

The time complexity of Algorithm 3 is $O(n^2t(n))$ and $\Omega(nt(n))$. The worst-case scenario occurs when adding n summands in the right-to-left order. In this case, BUILDSUBTREE will be invoked with all suffixes of $\{0, 1, \dots, n-1\}$, and $l^{i,j}$ for all $0 \leq i < j < n$ will be calculated. The worst-case time complexity is $\Theta(n^2t(n))$. In practice, this order is cache-unfriendly, and thus no library uses it.

The best-case scenario corresponds to the sequential summation, where the summation tree will be constructed in one pass, and only $l^{0,j}$ for all $0 < j < n$ will be calculated. The best-case time complexity is $\Theta(nt(n))$. In practice, many libraries use similar orders, because these orders are cache-friendly and efficient.

5.2 Adding support for matrix accelerators

5.2.1 Multi-term fused summation

Matrix accelerators such as NVIDIA Tensor Cores are specialized hardware components in modern GPUs. Matrix accelerators enable assembly instructions that take a matrix $A = (a_{ij})_{M \times K}$, a matrix $B = (b_{ij})_{K \times N}$, and a matrix $C = (c_{ij})_{M \times N}$ as input, and produce a matrix $D = (d_{ij})_{M \times N}$ such that $D = A \times B + C$. The data types of A and B are identical. The data types of C and D are also identical, and their precision is no lower than the precision of A and B .

The numerical behavior of these assembly instructions remains undisclosed. Specifically, the computation of $d_{ij} = c_{ij} + \sum_{k=0}^{K-1} a_{ik}b_{kj}$ is executed in an undocumented way. Through delicate numerical experiments, prior works [7, 16] have found that for double-precision input, the computation is executed in a chain of standard FMAs; for low-precision input (specifically, when the precision of A and B is lower than float32), the computation of $d_{ij} = c_{ij} + \sum_{k=0}^{K-1} a_{ik}b_{kj}$ is executed based on multi-term fused summation:

- The products are computed exactly, and the results are maintained in full precision without rounding after the multiplication.
- The summation of a group of summands is performed in a fixed-point manner. Specifically, the significands are aligned to the largest exponent of the summands, and then truncated to 24+ bits (i.e., no less than the precision of float32). The number of bits and the truncation method vary depending on the GPU architecture.
- Then, the sum is converted to the floating-point number in the output data type of the instruction.

Note that the size of the group w , the width of the accumulator, and the detailed conversion method vary depending on the GPU architecture. In addition, previous works do not target the high-level APIs and libraries, so the accumulation orders of them remains unknown.

Our proposed solutions can work for standard FMAs. However, multi-term fused summation requires a new method, because it is executed in a non-standard, IEEE-754-incompliant way. Specifically, in multi-term fused summation, w summands (e.g., $x_0 = c$, and $x_i = a_{i-1}b_{i-1}$ for $1 \leq i < w$) are summed in a fixed-point manner, thus making the result independent of the summation order. To represent this operation in the summation tree, we should use a node with w children instead of a node with two children. Therefore, the summation tree should be an w -way tree.

5.2.2 Constructing the multiway summation tree

To adapt to the multiway tree, we first revisit BasicFPRev in Section 4. The first two steps still work because we find that the key equation $l^{i,j} = n - \text{SUMIMPL}(A^{i,j})$ remains valid in multi-term fused summation. Thus, the values of $l^{i,j}$ can be

obtained in the same way, and we only need to redesign the tree construction algorithm in the third step.

Then, we revisit the tree construction algorithm in Algorithm 3. In `BUILDSUBTREE(I)`, we calculate $l^{i,j}$ for a fixed i and all $j \in I - \{i\}$, enumerate them in ascending order, and maintain r as the root of the largest constructed subtree containing node $\#i$. For some $l \in L_i = \{l^{i,j} : j \in I - \{i\}\}$ and $J_l = \{j : j \in I - \{i\} \wedge l^{i,j} = l\}$, the return value of `BUILDSUBTREE(J_l)` is the subtree with J_l as its leaf nodes. The root of this subtree must be the sibling node of r , so we can create a new node as their parent node and update r . However, this relation is not always true for the multiway tree.

In addition to being sibling node, the root of the subtree may also be the parent node of r in the multiway tree. For example, suppose a 5-way tree with leaf nodes $I = \{0, 1, 2, 3, 4\}$ as the children of the root. Then, when $r = 0$, $l = 5$, and $J_l = \{1, 2, 3, 4\}$, solving the subproblem for J_l should return a partial subtree with J_l as its leaves. The root node of the subtree is the parent node of r .

To distinguish the two cases, we observe the return value of `BUILDSUBTREE(J_l)`, denoted by T' , and the complete subtree rooted at the root of T' , denoted by T_c . In the first case, the root of T' should be the sibling of r , and $T' = T_c$. In the second case, the root of T' should be the parent of r , and $T' \subset T_c$. Therefore, we can compare the size of T' (denoted by $n_{\text{leaves}}^{T'}$) with the size of T_c (denoted by $n_{\text{leaves}}^{T_c}$). We note that $n_{\text{leaves}}^{T'} = |J_l|$, and $n_{\text{leaves}}^{T_c} = \max\{l^{j,k} : j, k \in J_l\} = \max(L_{\min(J_l)})$. Therefore, if $\max(L_{\min(J_l)}) = |J_l|$, then the root of T' should be the sibling of r , so we should create a new node as their parent node and update r with the index of this new node. Otherwise, $\max(L_{\min(J_l)}) > |J_l|$, so the root of T' should be the parent of r , and thus we should add an edge from r to the root of T' , and update r with the root.

Through this modification, the multiway tree can be correctly constructed. We elaborate on the above process in Algorithm 4, i.e., the algorithm of `FPREV`. It has the same time complexity as Algorithm 3 (note that Algorithm 3 just corresponds to the case where $\max(L_{\min(J_l)}) = |J_l|$), and supports multi-term fused summation.

5.3 Time complexity and correctness

The time complexity of `FPREV` is $O(n^2 t(n))$ and $\Omega(nt(n))$, following the same analysis in Section 5.1.3. The correctness of it is also guaranteed by design and can be proven following the same process in Section 4.4.

6 Case study

In this section, we apply `FPREV` to two prevalent numerical libraries: NumPy [9], the most popular Python library for numerical computing on CPUs, and PyTorch [22], a very popular Python library for numerical computing on GPUs. We

Algorithm 4 The algorithm of `FPREV`.

Require: Implementation `SUMIMPL` and the number of summands n

Ensure: Summation tree of `SUMIMPL`

function `FPREV(SUMIMPL, n)`

function `BUILDSUBTREE(I)`

$T \leftarrow \emptyset$

if $|I| = 1$ **then** ▷ stop condition

return T

$i \leftarrow \min(I); L_i \leftarrow \emptyset$

for $j \in I - \{i\}$ **do** ▷ calculate $l^{i,j}$ on demand

$A^{i,j} \leftarrow (1, 1, \dots, 1); A_i^{i,j} \leftarrow M; A_j^{i,j} \leftarrow -M$

$l^{i,j} \leftarrow n - \text{SUMIMPL}(A^{i,j})$

$L_i \leftarrow L_i \cup \{l^{i,j}\}$

$r \leftarrow i$ ▷ current root of the subtree

for $l \in L_i$ in ascending order **do**

$J_l \leftarrow \{j : j \in I - \{i\} \wedge l^{i,j} = l\}$

$(T', n_{\text{leaves}}^{T'}) \leftarrow \text{BUILDSUBTREE}(J_l)$

$T \leftarrow T \cup T'$

if $|J_l| = n_{\text{leaves}}^{T_c}$ **then** ▷ $T' = T_c$

$T \leftarrow T \cup \{(r, r+n), (\text{GetRoot}(T'), r+n)\}$

$r \leftarrow r+n$

else ▷ $T' \subset T_c$

$T \leftarrow T \cup \{(r, \text{GetRoot}(T'))\}$

$r \leftarrow \text{GetRoot}(T')$

return $(T, \max(L_i))$

$(T, n_{\text{leaves}}^{T_c}) \leftarrow \text{BUILDSUBTREE}(\{0, 1, \dots, n-1\})$

return T

successfully identify and analyze the undocumented accumulation orders in these libraries.

6.1 NumPy's implementation on CPUs

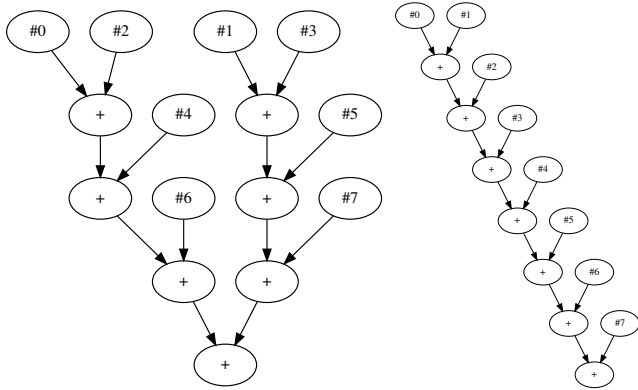
We use `FPREV` to test NumPy (version 1.26) on three CPUs:

- CPU-1: Intel Xeon E5-2690 v4 (24 v-cores)
- CPU-2: AMD EPYC 7V13 (24 v-cores)
- CPU-3: Intel Xeon Silver 4210 (40 v-cores)

Summation. On these CPUs, we find that NumPy implements identical accumulation order for the summation function in single precision. Therefore, NumPy's summation is verified to be reproducible across these systems, and can be used in software requiring numerical reproducibility.

The accumulation order is sequential for $n < 8$. For $8 \leq n \leq 128$, NumPy implements an eight-way summation. Each way i sums up $a_i, a_{i+8}, a_{i+16}, \dots$ sequentially, and the sums of eight ways are summed using pairwise summation. For example, Figure 1 shows the accumulation order for $n = 32$. This accumulation order implies that developers can leverage the eight-way SIMD instructions in the CPU to accelerate computation. For $n > 128$, NumPy increases the number of ways, thus leveraging multi-threading for large-scale summation.

Other AccumOps. We also test NumPy’s dot product, matrix-vector multiplication, and matrix multiplication functions in single precision. We observe discrepancies in the accumulation order across the tested CPUs. For example, Figure 3 shows the accumulation orders of NumPy’s $n \times n$ matrix-vector multiplication for $n = 8$ on the CPUs. We note that on CPU-1 and CPU-2, the 32 products of each output element are accumulated using 2-way summation, whereas on CPU-3, which has more cores than CPU-1 and CPU-2, the products are accumulated sequentially.



(a) On Intel Xeon E5-2690 v4 and AMD EPYC 7V13 (24 v-cores). (b) On Intel Xeon Silver 4210 (40 v-cores).

Figure 3: The accumulation orders of NumPy’s 8×8 matrix-vector multiplication on different CPUs.

In summary, NumPy’s summation function is safe for developing reproducible software for these CPUs, while other AccumOps of NumPy should not be used in software requiring numerical reproducibility.

6.2 PyTorch’s implementation on GPUs

We use FPRev to test PyTorch (version 2.3) on three GPUs:

- GPU-1: NVIDIA V100 (5120 CUDA cores)
- GPU-2: NVIDIA A100 (6912 CUDA cores)
- GPU-3: NVIDIA H100 (16896 CUDA cores)

On these GPUs, we observe findings similar to those for NumPy: PyTorch implements identical accumulation orders for the summation function in single precision but not for the BLAS operations. Therefore, PyTorch’s summation function is safe for developing reproducible software for these GPUs, while other AccumOps of PyTorch should not be used in software requiring numerical reproducibility.

Matrix multiplication on Tensor Cores. To enable Tensor Core computation, we apply FPRev to half-precision matrix multiplication in PyTorch, which is implemented using the cuBLAS backend. The results show that the summation tree is a 5-way tree on NVIDIA V100, a 9-way tree on A100, and a 17-way tree on H100, corroborating the conclusion in [7, 16], which states that the Tensor Cores on NVIDIA Volta, Ampere,

and Hopper architectures use (4+1)-, (8+1)-, and (16+1)-term fused summation respectively. For example, Figure 4 shows the summation trees for $n = 32$ on these devices.

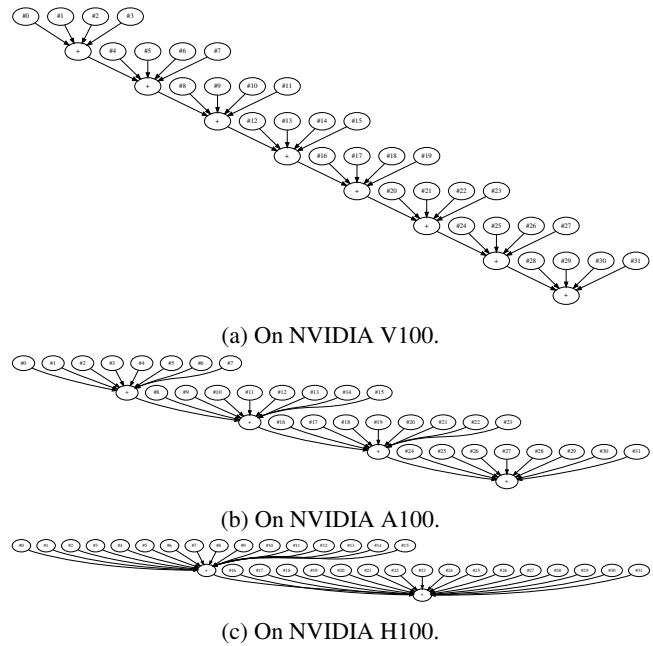


Figure 4: The accumulation orders of PyTorch’s $32 \times 32 \times 32$ matrix multiplication on Tensor Cores.

We also examine the SASS assembly instructions they use, and observe that V100 uses the `HMMMA.884` instruction, and both A100 and H100 use the `HMMMA.16816` instruction. **Interestingly, an `HMMMA.16816` instruction on A100 indicates the shape of the inputs where the accumulation dimension $K = 16$, but it is implemented through (8+1)-term fused summation by the A100 Tensor Core hardware.**

7 Performance evaluation

7.1 Experiment design

In this section, we evaluate the efficiency of FPRev. Specifically, we aim to answer the following research questions (RQs):

- RQ1: how efficient is FPRev when applied to different libraries?
- RQ2: how efficient is FPRev when applied to different operations?
- RQ3: how efficient is FPRev on different CPUs and GPUs?

To answer the RQs, we measure the run time (wall-clock time) of applying our solutions to tested libraries and operations. We implement FPRev (Algorithm 4) in Python (version 3.11). For comparison, we also implement the basic solution (Algorithm 2), denoted by BasicFPRev.

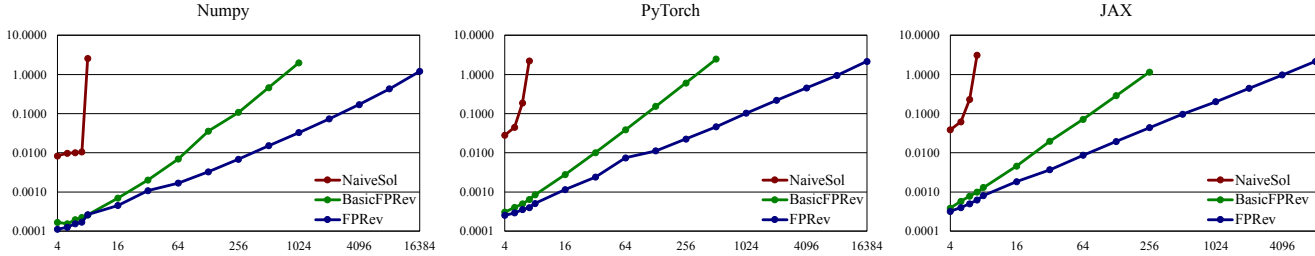


Figure 5: Run time of applying NaiveSol, BasicFPRRev, and FPRRev to the summation functions in NumPy, PyTorch, and JAX. The vertical axis represents run time in seconds. The horizontal axis represents the number of summands n .

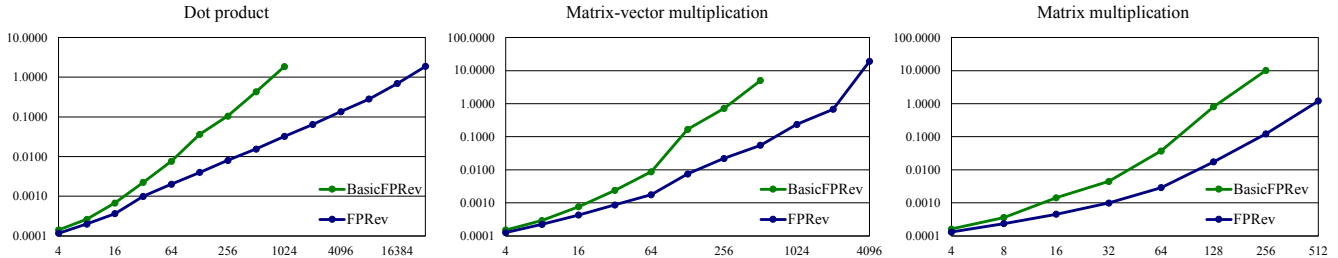


Figure 6: Run time of applying BasicFPRRev and FPRRev to the dot product, matrix-vector multiplication, and matrix multiplication functions in NumPy. The vertical axis represents run time in seconds. The horizontal axis represents the number of summands n .

7.2 RQ1: How efficient is FPRRev when applied to different libraries?

For RQ1, we test the single-precision summation function in three libraries: NumPy (version 1.26) [9], PyTorch (version 2.3) [22], and JAX (version 0.4) [3]. We run the experiments on Intel Xeon E5-2690 v4 with 24 v-cores. In these experiments, we also implement the naive brute-force solution (Section 3.3), denoted as “NaiveSol”, to show its extremely low efficiency. For remaining RQs, we omit the naive solution because it is proven to be too inefficient.

We begin with the number of summands $n = 4$, and increment n until the run time exceeds one second. Each experiment is carried out 10 times, and the arithmetic mean of the 10 results is reported in Figure 5. The red curves indicate that the run time of NaiveSol grows exponentially as n grows. The results substantiate the $O(4^n/n^{3/2} \cdot t(n))$ time complexity of NaiveSol. The green and blue lines show that the run time of BasicFPRRev and FPRRev grows polynomially. The different slopes also demonstrate that the run time of BasicFPRRev is longer than that of FPRRev, and increases more rapidly as n increases. This is because the time complexity of BasicFPRRev is $\Theta(n^2 t(n))$, while that of FPRRev is $\Omega(nt(n))$ and $O(n^2 t(n))$.

These trends suggest that the scalability of BasicFPRRev is much better than that of NaiveSol, and the scalability of FPRRev is even better. For example, when $n = 16$, NaiveSol can take over 24 hours to produce an output, but BasicFPRRev and FPRRev only take less than 0.01 seconds. If $n = 8192$, BasicFPRRev will take over 100 seconds to produce an output,

but FPRRev only takes about 1 second.

7.3 RQ2: How efficient is FPRRev when applied to different operations?

For RQ2, we test the single-precision dot product, matrix-vector multiplication, and matrix multiplication functions in NumPy on Intel Xeon E5-2690 v4. The time complexity of these functions is $O(n)$, $O(n^2)$, and $O(n^3)$, respectively.

Similarly, we begin with $n = 4$, and increment n until the run time exceeds one second. Each experiment is carried out 10 times, and the arithmetic mean of the 10 results is reported in Table 6. The different slopes indicate that the time complexity of BasicFPRRev is higher than that of FPRRev. In addition, as the time complexity of the workload increases, the growth speed of the runtime with regard to n accelerates. Therefore, the speedup of FPRRev over BasicFPRRev is more pronounced as the workload is more complex. For example, for $n = 256$, FPRRev is 13.0 \times as fast as BasicFPRRev for dot product, 32.3 \times for matrix-vector multiplication, and 82.1 \times for matrix multiplication.

7.4 RQ3: How efficient is FPRRev on different CPUs and GPUs?

For RQ3, we test the single-precision matrix multiplication in PyTorch on the CPUs and GPUs listed in Section 6. Similarly, we begin with $n = 4$, and increment n until the run

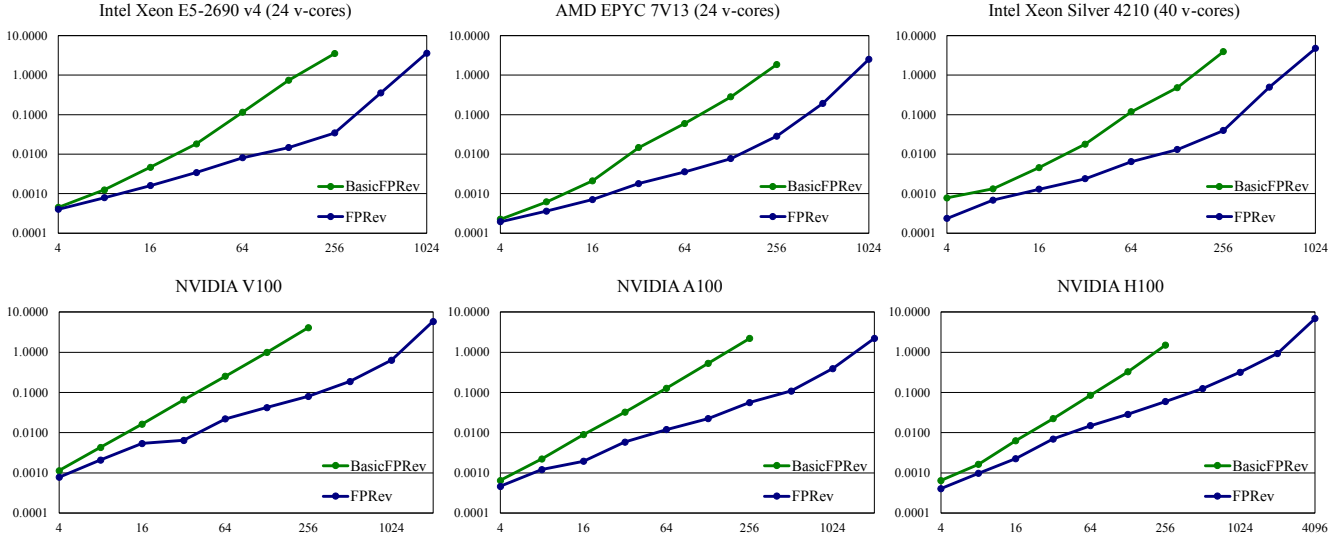


Figure 7: Run time of applying BasicFPRRev and FPRRev to the matrix multiplication functions in PyTorch on different CPUs and GPUs. The vertical axis represents run time in seconds. The horizontal axis represents the number of summands n .

time exceeds one second. Each experiment is carried out 10 times, and the arithmetic mean of the 10 results is reported in Figure 7. The results demonstrate consistent improvements in the runtime of FPRRev compared to BasicFPRRev. Therefore, FPRRev is consistently more efficient than BasicFPRRev on different devices.

8 Discussion

8.1 Threats to validity

Internal. The precision of the floating-point data type can limit the validity of FPRRev. For float32, which has a precision of 24 bits, the maximum number of summands (n) that FPRRev supports is $2^{24} + 1 = 16777217$. For larger numbers, the sum of $n - 2$ ones cannot be represented precisely by float32, so the sum of masked all-one arrays may be incorrect. This problem could be solved by dynamically replacing the multiple ones corresponding to a constructed subtree with their sum and multiple zeros. This solution does not affect efficiency.

For low-precision data types, there is an additional issue of the floating-point swamping because $M \ll n$ may not hold. For example, the maximum exponent of float16 is 15. If $M = 2^{15}$ and $\mu = 256$, $\pm M + \mu \neq \pm M$. To solve this problem, we can replace the ones in the masked all-one arrays with smaller numbers (e.g., 2^{-24}), and scale the sum back to an integer between 0 and $n - 2$ when calculating $l^{i,j}$. This solution does not affect efficiency, either.

External. If the tested implementation has functional defects, FPRRev may not yield the correct result. Nonetheless, we can still extract some diagnostic information from the abnormal output of FPRRev. For example, if a conversion from

float64 to float32 occurs during summation, FPRRev will detect overflows, indicating the presence of the conversion.

8.2 Extensibility

Section 6 has demonstrated that FPRRev can be applied to most popular numerical libraries. FPRRev can be applied to other implementations as long as they fall within the scope detailed in Section 3. FPRRev will also work for collective communication primitives if their accumulation order is predetermined. To further extend our tool to other functions based on special summation algorithms, the algorithms must satisfy the property $l^{i,j} = n - \text{SUMIMPL}(A^{i,j})$. Thus, our methods can be abstracted into a template to reveal the accumulation order.

9 Conclusion

In this paper, we introduce FPRRev, a diagnostic tool for revealing the accumulation order in software and hardware implementations through numerical testing. It can help verify and facilitate the development of reproducible software. As a case study, FPRRev reveal the undisclosed accumulation orders of prevalent numerical libraries such as NumPy and PyTorch on different CPUs and GPUs. We also demonstrated the efficiency FPRRev through experiments covering various implementations and devices. Our source code will be made available after the double-blind review process, encouraging further investigation and improvement by the research community.

References

- [1] Andrea Arteaga, Oliver Fuhrer, and Torsten Hoefler. Designing Bit-Reproducible Portable High-Performance Applications. In *IEEE International Parallel and Distributed Processing Symposium (IPDPS)*, pages 1235–1244, 2014. doi:10.1109/IPDPS.2014.127.
- [2] David H Bailey, Jonathan M Borwein, and Victoria Stodden. Facilitating reproducibility in scientific computing: Principles and practice. In *Reproducibility: Principles, Problems, Practices, and Prospects*, pages 205–231. Wiley Online Library, 2016. Publisher: Wiley Online Library.
- [3] James Bradbury, Roy Frostig, Peter Hawkins, Matthew James Johnson, Chris Leary, Dougal Maclaurin, George Necula, Adam Paszke, Jake VanderPlas, Skye Wanderman-Milne, and Qiao Zhang. JAX: composable transformations of Python+NumPy programs, 2018. URL: <http://github.com/google/jax>.
- [4] Sylvain Collange, David Defour, Stef Graillat, and Roman Iakymchuk. Numerical Reproducibility for the Parallel Reduction on Multi- and Many-Core Architectures. *Parallel Computing*, 49:83–97, 2015. doi:10.1016/j.parco.2015.09.001.
- [5] James Demmel and Hong Diep Nguyen. Fast Reproducible Floating-Point Summation. In *IEEE Symposium on Computer Arithmetic (ARITH)*, pages 163–172, 2013. doi:10.1109/ARITH.2013.9.
- [6] James Demmel and Hong Diep Nguyen. Parallel Reproducible Summation. *IEEE Transactions on Computers*, 64(7):2060–2070, 2015. doi:10.1109/TC.2014.2345391.
- [7] Massimiliano Fasi, Nicholas J. Higham, Mantas Mikaitis, and Srikara Pranesh. Numerical behavior of NVIDIA tensor cores. *PeerJ Computer Science*, 7:e330, 2021. doi:10.7717/peerj-cs.330.
- [8] Hui Guo, Ignacio Laguna, and Cindy Rubio-González. pLiner: isolating lines of floating-point code for compiler-induced variability. In *International Conference for High Performance Computing, Networking, Storage and Analysis (SC)*, page 49, 2020. doi:10.1109/SC41405.2020.00053.
- [9] Charles R. Harris, K. Jarrod Millman, Stéfan van der Walt, Ralf Gommers, Pauli Virtanen, David Cournapeau, Eric Wieser, Julian Taylor, Sebastian Berg, Nathaniel J. Smith, Robert Kern, Matti Picus, Stephan Hoyer, Marten H. van Kerkwijk, Matthew Brett, Allan Haldane, Jaime Fernández del Río, Mark Wiebe, Pearu Peterson, Pierre Gérard-Marchant, Kevin Sheppard, Tyler Reddy, Warren Weckesser, Hameer Abbasi, Christoph Gohlke, and Travis E. Oliphant. Array programming with NumPy. *Nature*, 585:357–362, 2020. URL: <https://doi.org/10.1038/s41586-020-2649-2>, doi:10.1038/s41586-020-2649-2.
- [10] Yun He and Chris H. Q. Ding. Using Accurate Arithmetics to Improve Numerical Reproducibility and Stability in Parallel Applications. *The Journal of Supercomputing*, 18(3):259–277, 2001. doi:10.1023/A:1008153532043.
- [11] Nicholas J. Higham. The Accuracy of Floating Point Summation. *SIAM Journal on Scientific Computing*, 14(4):783–799, 1993. doi:10.1137/0914050.
- [12] IEEE. *IEEE Standard for Floating-Point Arithmetic*, 2019. doi:10.1109/IEEESTD.2019.8766229.
- [13] Intel Corporation. *Intel Math Kernel Library*. URL: <https://www.intel.com/content/www/us/en/developer/tools/oneapi/onemkl.html>.
- [14] Ignacio Laguna. Varity: Quantifying Floating-Point Variations in HPC Systems Through Randomized Testing. In *IEEE International Parallel and Distributed Processing Symposium (IPDPS)*, pages 622–633, 2020. doi:10.1109/IPDPS47924.2020.00070.
- [15] Siu Kwan Lam, Antoine Pitrou, and Stanley Seibert. Numba: a LLVM-based Python JIT compiler. In *Workshop on the LLVM Compiler Infrastructure in HPC (LLVM-HPC)*, pages 7:1–7:6. ACM, 2015. doi:10.1145/2833157.2833162.
- [16] Xinyi Li, Ang Li, Bo Fang, Katarzyna Swirydowicz, Ignacio Laguna, and Ganesh Gopalakrishnan. FTTN: Feature-Targeted Testing for Numerical Properties of NVIDIA & AMD Matrix Accelerators. In *IEEE/ACM International Symposium on Cluster, Cloud and Internet Computing (CCGRID)*, pages 39–46. IEEE, 2024. URL: <https://doi.org/10.1109/CCGrid59990.2024.00014>, doi:10.1109/CCGRID59990.2024.00014.
- [17] Stefano Markidis, Steven Wei Der Chien, Erwin Laure, Ivy Bo Peng, and Jeffrey S. Vetter. NVIDIA Tensor Core Programmability, Performance & Precision. In *IEEE International Parallel and Distributed Processing Symposium (IPDPS) Workshops*, pages 522–531. IEEE Computer Society, 2018. doi:10.1109/IPDPSW.2018.00091.
- [18] Dolores Miao, Ignacio Laguna, and Cindy Rubio-González. Expression Isolation of Compiler-Induced Numerical Inconsistencies

- in Heterogeneous Code. In *ISC High Performance*, pages 381–401, 2023. URL: https://doi.org/10.1007/978-3-031-32041-5_20, doi:10.1007/978-3-031-32041-5_20.
- [19] NVIDIA. *Parallel Thread Execution ISA*. URL: <https://docs.nvidia.com/cuda/parallel-thread-execution/>.
- [20] NVIDIA Corporation. *cuBLAS: Basic Linear Algebra on NVIDIA GPUs*. URL: <https://developer.nvidia.com/cublas/>.
- [21] OpenBLAS Contributors. *OpenBLAS: An optimized BLAS library*. URL: <https://www.openblas.net/>.
- [22] Adam Paszke, Sam Gross, Francisco Massa, Adam Lerer, James Bradbury, Gregory Chanan, Trevor Killeen, Zeming Lin, Natalia Gimelshein, Luca Antiga, Alban Desmaison, Andreas Köpf, Edward Z. Yang, Zachary DeVito, Martin Raison, Alykhan Tejani, Sasank Chilamkurthy, Benoit Steiner, Lu Fang, Junjie Bai, and Soumith Chintala. PyTorch: An Imperative Style, High-Performance Deep Learning Library. In *Conference on Neural Information Processing Systems (NeurIPS)*, pages 8024–8035, 2019. URL: <https://proceedings.neurips.cc/paper/2019/hash/bdbca288fee7f92f2bfa9f7012727740-Abstract.html>.
- [23] Christophe Pérignon, Olivier Akmansoy, Christophe Hurlin, Anna Dreber, Felix Holzmeister, Jürgen Huber, Magnus Johannesson, Michael Kirchler, Albert J Menkveld, Michael Razen, et al. Computational reproducibility in finance: Evidence from 1,000 tests. *The Review of Financial Studies*, 37(11):3558–3593, 2024.
- [24] Gary Polhill, Luis Izquierdo, and Nick Gotts. The ghost in the model (and other effects of floating point arithmetic). *Journal of Artificial Societies and Social Simulation*, 8(1), 2004.
- [25] Md Aamir Raihan, Negar Goli, and Tor M. Aamodt. Modeling Deep Learning Accelerator Enabled GPUs. In *IEEE International Symposium on Performance Analysis of Systems and Software (ISPASS)*, pages 79–92, 2019. doi:10.1109/ISPASS.2019.00016.
- [26] Robert Endre Tarjan and Jan van Leeuwen. Worst-case Analysis of Set Union Algorithms. *Journal of the ACM*, 31(2):245–281, 1984. doi:10.1145/62.2160.
- [27] Michela Taufer, Omar Padron, Philip Saponaro, and Sandeep Patel. Improving numerical reproducibility and stability in large-scale numerical simulations on GPUs. In *IEEE International Parallel and Distributed Processing Symposium (IPDPS)*, pages 1–9, 2010. doi:10.1109/IPDPS.2010.5470481.
- [28] Philippe Tillet, Hsiang-Tsung Kung, and David D. Cox. Triton: an intermediate language and compiler for tiled neural network computations. In *ACM SIGPLAN International Workshop on Machine Learning and Programming Languages*, pages 10–19. ACM, 2019. doi:10.1145/3315508.3329973.
- [29] Oreste Villa, Daniel Chavarria-Miranda, Vidhya Guru-moorthi, Andrés Márquez, and Sriram Krishnamoorthy. Effects of floating-point non-associativity on numerical computations on massively multithreaded systems. In *Cray User Group Meeting (CUG)*, volume 3, 2009.